[UCI]I804:24011-200000276172

2014년 8월

석사학위논문

Determination of the Recovery Time of Unhealthy SISs in LOCA

조 선 대 학 교 대 학 원

원 자 력 공 학 과

김 대 섭

Determination of the Recovery Time of Unhealthy SISs in LOCA

LOCA에서 불건전한 안전주입시스템의 회복시간의 결정

2014년 8월 25일

조 선 대 학 교 대 학 원

원 자 력 공 학 과

김 대 섭

Determination of the Recovery Time of Unhealthy SISs in LOCA

지도교수 나 만 균

이 논문을 공학 석사학위신청 논문으로 제출함

2014년 8월

조 선 대 학 교 대 학 원

원 자 력 공 학 과

김 대 섭

김대섭의 석사학위 논문을 인준함

위원장 조선대학교 교 수 이 경 진 (인)

위 원 조선대학교 교 수 송 종 순 (인)

위 원 조선대학교 교 수 나 만 균 (인)

2014년 8월

조 선 대 학 교 대 학 원

CONTENTS

List of Figures

List of Tables

초　　록

LOCA에서 불건전한 안전주입시스템의 회복시간의 결정

김 대 섭
지도 교수 : 나 만 균
원자력공학과
조선대학교 대학원

최근 일본 후쿠시마 원전 사고에서 보듯이 중대사고시 노내 상태를 정확히 알아내지 못하는 상황에 처하게 되어 사고 평가 및 결과를 전혀 예측하지 못하는 상황에 도달하게 되었다. 원자로 상태를 정확히 알 수 없어 이것은 사고회복을 위한 초기 대응 실패로 연결되었으며, 사고를 조기에 마무리하고 원자로가 안정 저온정지에 도달할 기회를 상실하게 되었다. 본 연구는 원전 사고시 사고회복을 위한 인공지능 방법론의 적용 가능성을 검토하고, 이를 이용한 LOCA에서의 안전주입계통의 작동에 대한 사고 회복 시간을 결정하기 위하여 수행되었다. 이에 따라 본 연구에서는 다양한 인공지능 기법(Group Method of Data Handling: GMDH, Fuzzy Neural Network: FNN, Support Vector Machine: SVM 등)을 이용한 방법론을 검토하였으며 [1-4], 사고 관리를 적절히 수행하지 못하는 초기사건이나 안전계통이 적절히 작동하지 못한 경우 LOCA 시나리오 예측에 적용하였다. 이전 연구에서 중대사고 시나리오 전개과정의 특정 시점을 예측하기 위하여 GMDH와 FNN 모델을 적용하여, 선택된 입력 변수와 최대 예측 오차 및 RMS 오차를 분석한 결과, GMDH와 FNN 모델은 정확히 LOCA의 시나리오를 예측할 수 있었다. 본 연구에서는 안전주입계통의 작동여부 (실패 또는 정상작동 또는 지연작동)에 따라 중대 사고를 나타내는 주요한 시점의 변화를 분석하였다.

예측 모델은 학습 데이터를 이용하여 개발 하고 독립적인 시험 데이터를 이용하여 검증을 수행하였으며, 모델 개발과 검증을 위한 DB는 MAAP4 [12]코드를 이용하여 한국표준형원전 (OPR1000)을 대상으로 하는 시뮬레이션을 통해 구축하였다. 사고모의는 고압안전주입과 저압안전주입으로 나누어서 파단 크기별로 실행하여 사고회복 시

간을 결정하였다. 단, 격납용기 살수 계통과 재순환 모드는 정상적으로 작동하였다고 가정하였다. 시뮬레이션 결과, 배관 파단크기별로 중대사고 시나리오를 나타내는 주요 시점(노심 노출, 압력용기 손상)에 도달하지 않도록 안전주입계통의 사고 회복 시간을 결정할 수 있었다.

안전계통의 작동여부에 따라 원자로 상태를 확인하는 것은 매우 중요하다. OPR1000을 대상으로 하는 시뮬레이션을 통해 안전주입시스템의 작동에 따라 사고회복을 위한 시간을 결정할 수 있었다. 또한, 압력과 지연작동과 같이 안전계통의 적절한 운전에 간섭하는 요소를 알 수 있었다. 원자력 발전소에서 냉각재 상실 사고 발생시 GMDH 모델을 통하여 LOCA의 파단크기 및 시나리오를 나타내는 주요한 시점을 정확히 예측한다면 안전주입시스템의 사고 회복 결정시간에 따라 중대 사고를 효과적으로 관리할 수 있을 것으로 기대된다.

Ⅰ. Introduction

When operators do not exactly know the inner conditions of a reactor during severe accidents such as the Fukushima NPP accident in Japan, it is hard to predict the accident progress and the results. Furthermore, it is necessary to develop safety measures for the worst conditions such as natural disasters, terrorism, etc. Therefore, the NPP accident recovery aid system is necessary to achieve stable shutdown from Design Basis Accidents (DBA).

To predict the recovery time of safety system, it is regarded to classify the initial event, and predict the important timings for severe accident scenarios. It is very important to measure the safety-related parameters for a very short period in the initial event conditions that can lead to a serious accident, such as a loss of coolant accident (LOCA) and steam generator tube rupture (SGTR).

In previous papers [1-4], a fuzzy neural network (FNN) and group method of data handling (GMDH) models were proposed to predict the severe accident scenario, which has a direct impact on the important times (time approaching the core exit temperature exceeding 1200°F, core uncovery time, reactor vessel failure time, etc.).

In this thesis, the changes of important timings for severe accident scenarios (core uncovery, reactor vessel failure, etc.) have been analyzed according to the Safety Injection System (SIS) status (no actuation, normal actuation, delayed actuation) as part of the successful control path analysis from DBA for the composition of accident recovery aid system.

These data were obtained by simulating severe accident scenarios for the Optimized Power Reactor 1000 (OPR1000) using the MAAP4 code [12]. Simulations were conducted according to break size (0.1%, 1%, … , 100%), and high pressure and low pressure SIS actuation status. It was assumed that Containment Spray System (CSS), Safety Injection Tank (SIT) and Recirculation (REC) mode were normally actuated.

To check the inner conditions of the reactor is very important, depending on the actuation status of the safety systems. We confirmed an alteration of significant timing according to the state within the safety injection system through the simulation of OPR1000. Also, we could find the elements that interfere with the proper operation of the safety system such as pressure and time delay. If the GMDH model has the capability to accurately predict LOCA break size and important timing for severe accident scenarios (core uncovery, reactor vessel failure, etc.), it is possible to determine the recover time of the safety injection systems for preventing the core uncovery and RV failure.

Ⅱ. Prediction of the LOCA Scenarios

A. FNN (Fuzzy Neural Network) Method

1. Fuzzy Inference Model

A fuzzy inference model consists of situation and action pairs where conditional rules described in if then statements are generally used. The task of adapting fuzzy systems for on-line application involves neuronal improvements of fuzzy inference systems and the fuzzification of neural network systems. In this way we can exploit the complementary nature of fuzzy inference systems and neural network systems. The combination of the two systems is usually called an FNN system [5].

The fuzzy inference model can be accomplished through a clustering of numerical data. A cluster center is in essence a prototypical data point that exemplifies a characteristic behavior of a target system, and each cluster center can be used as the basis of a fuzzy rule that describes the system behavior. The development of a complete fuzzy system identification algorithm can therefore be based on the results of a subtractive clustering (SC) technique; this type of technique can be used as the basis of a fast and robust algorithm for identifying a fuzzy inference model. We therefore present a fuzzy inference model based on an SC method, and the model can be used to predict the residual stress of dissimilar metal welding [6].

The data-based fuzzy inference model assumes the availability of N input/output training data pairs $(\boldsymbol{x}^T(k), y(k))$, where $\boldsymbol{x}^T(k) = (x_1(k), x_2(k), \cdots, x_m(k))$, $k = 1, 2, \ldots, N$. If we assume that the data points have been normalized in each dimension, the method can begin by generating a number of clusters in the $m \times N$ dimensional input space. To develop a systematic approach to the generation of fuzzy rules from a given input-output data set, we can use a Takagi-Sugeno-type fuzzy inference model, where the i-th fuzzy rule for the k-th time instant data is formulated as follows [6]:

$$If\ \ x_1(k)\ \ is\ \ A_{i,1}(k)\ \ AND\ \ \cdots\ \ AND\ \ x_m(k)\ \ is\ \ A_{i,m}(k), \tag{1}$$
$$then\ \ \hat{y_i}(k)\ \ is\ \ f_i(x_1(k),\ \cdots,\ x_m(k))$$

where $x_j(k)$ is the input linguistic variable to the fuzzy inference model ($j=1,2,\ldots,m$; $m=$ the number of input variables), $A_{i,j}(k)$ is the membership function of the j-th input variable for the i-th fuzzy rule($i=1,2,\ldots,n$; $n=$ the number of rules), and $\hat{y_i}(k)$ is the output of the i-th fuzzy rule.

Like two methods which were mentioned previously, the SC method is applied to obtain the informative training data. And when the cluster estimation method is applied to a collection of input/output data, we can generate a number of n Takagi-Sugeno-type fuzzy rules, where the premise parts are fuzzy sets defined by the cluster centers that are obtained by the SC algorithm. The membership function value, $A_i(\boldsymbol{x}(k))$, of an input data vector, $\boldsymbol{x}(k)$, to the i-th cluster center, $\boldsymbol{x}_c(i)$, can be defined as follows:

$$A_i(\boldsymbol{x}(k)) = e^{-4\,\|\,\boldsymbol{x}(k)-\boldsymbol{x}_c(i)\,\|\,^2/r_\alpha^2}. \tag{2}$$

The fuzzy inference model output, $\hat{y_i}(k)$, is calculated by the weighted average of the consequent parts of the fuzzy rules as follows:

$$\hat{y}(k)\frac{\sum_{i=1}^{n}A_i(\boldsymbol{x}(k))f_i(\boldsymbol{x}(k))}{\sum_{i=1}^{n}A_i(\boldsymbol{x}(k))}. \tag{3}$$

The function $f_i(\boldsymbol{x}(k))$ is a polynomial in the input variables, but it can be any function as long as it can appropriately describe the output of the fuzzy inference system within the fuzzy region specified by the antecedent of the rule. In the Takagi-Sugeno-type [5] fuzzy inference model, the output of an arbitrary i-th fuzzy rule, f_i, is usually represented by the following first-order polynomial of inputs:

$$f_i(\boldsymbol{x}(k)) = \sum_{j=1}^{m} q_{i,j} x_j(k) + r_i, \tag{4}$$

where $q_{i,j}$ is a weighting value of the j-th input on the i-th fuzzy rule output and r_i is a bias of the i-th fuzzy rule output.

The output of the fuzzy inference model given by Eq. (3) can therefore be rewritten as

$$\hat{y}(k) = \sum_{i=1}^{n} \overline{w_i} f_i(\boldsymbol{x}(k)) = \boldsymbol{w}^T(k)\boldsymbol{q}, \tag{5}$$

where

$$\overline{w_i}(k) = \frac{A_i(\boldsymbol{x}(k))}{\sum_{i=1}^{n} A_i(\boldsymbol{x}(k))},$$

$\boldsymbol{q} = [q_{1,1} \cdots q_{n,1} \cdots\cdots q_{1,m} \cdots q_{n,m}\ r_1 \cdots r_n]^T$, and

$\boldsymbol{w}(k) = [\overline{w_1}(k)x_1(k) \cdots \overline{w_n}(k)x_1(k) \cdots\cdots \overline{w_1}(k)x_m(k) \cdots \overline{w_n}(k)x_m(k)\ \ \overline{w_1}(k) \cdots \overline{w_n}(k)]^T$,
$k = 1, 2, \cdots, N$.

The value $\overline{w}_i(k)$ represents the normalized compatibility grade of the i-th fuzzy rule and consists of the input data and the normalized membership function values. The vector $\boldsymbol{q}$ is called the consequent parameter vector. Figure 1 describes the calculation procedure of the FNN model.

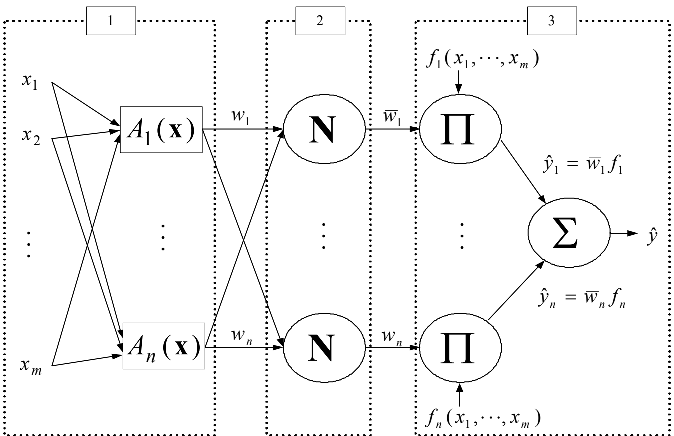

Fig. 1. A fuzzy neural network model

2. Training of the Fuzzy Inference Models

To attain the desired performance, the fuzzy inference system should be optimized by adapting the antecedent parameters (membership function parameters) and the consequent parameters (the polynomial coefficients of the consequent part).

The genetic algorithm that has recently been widely used as an optimization method assumes the form of starting from many search points simultaneously climbing many peaks in parallel. That algorithm is therefore less susceptible to being stuck at local optimum than conventional search methods. Moreover, the genetic algorithm is the most useful method of solving optimization problems with multiple objectives. However, because the genetic algorithm requires much computational time if there are many parameters involved, we can combine the genetic algorithm with a least squares algorithm to reduce the number of parameters that need to be optimized by the genetic algorithm. The genetic algorithm is used to optimize the cluster radii r_α and r_b as a means of generating the membership function through the SC of the numerical data; it also optimizes the other cluster radii of the SC which was explained in SVR as a means of sampling the training data from all the acquired data. The least squares algorithm is used to calculate the consequent parameters $q_{i,j}$ and r_i.

In genetic algorithms, the term chromosome refers to a candidate solution that minimizes a cost function and the candidate solution is generally encoded as a bit string. The bit strings for each chromosome include the two cluster radii, r_α and r_b, for the membership function generation and other two cluster radii for sampling of the training data; note also that the bit strings are encoded with binary bits. As the generation proceeds, the chromosome populations are iteratively altered by biological mechanisms inspired by natural evolution, such as selection, crossover, and mutation.

The genetic algorithms require a fitness function that assigns a score to each chromosome (candidate solution) in the current population; they also maximize the fitness function value. The fitness function evaluates the extent to which each candidate solution is suitable for specified objectives. A root mean square (RMS) error and a maximum error can be a measure of the estimation performance of the FNN model. However, the minimization of the errors may only induce the overfitting in the FNN model, which means that the FNN model is a good fit for a specific data set (the training data) but not for another data set. We therefore divided the acquired data into three kinds of data sets: the training data, the optimization data, and the test data. The training data are used to solve the antecedent parameters and the consequent parameters of the FNN models. The optimization data are used to improve generalization capability of the FNN model by using another independent data set. We used the test data to verify the developed FNN models. Our specified multiple objectives were to minimize the RMS error along with the small maximum error.

If the antecedent parameters of the FNN model are fixed by the genetic algorithm, the output of the resulting FNN model can be described as a series of expansions of some basis functions. The basis function expansion is linear in its adjustable parameters, as shown in Eq. (5), because $\boldsymbol{w}^T(k)$ is known by the genetic algorithm. Thus, we can use the least squares method to determine the consequent parameters. The consequent parameter $\boldsymbol{q}$ was chosen to minimize the following cost function, including the squared error between the target output $\boldsymbol{y}$ and the estimated output $\hat{\boldsymbol{y}}$:

$$J = \sum_{k=1}^{N_t} (y(k) - \hat{y}(k))^2 = \sum_{k=1}^{N_t} (y(k) - \boldsymbol{w}^T(k)\boldsymbol{q})^2 = \frac{1}{2}(\boldsymbol{y} - \hat{\boldsymbol{y}})^2, \tag{6}$$

where

$\boldsymbol{y} = [y(1)\ y(2) \cdots\ y(N_t)]^T$ and $\hat{\boldsymbol{y}} = [\hat{y}(1)\ \hat{y}(2) \cdots\ \hat{y}(N_t)]^T$.

The solution for minimizing the above cost function can be obtained by

$$\boldsymbol{y} = \hat{\boldsymbol{y}} = \boldsymbol{W}\boldsymbol{q}, \tag{7}$$

where

$\boldsymbol{W} = [\boldsymbol{w}(1)\, \boldsymbol{w}(2) \cdots\ \boldsymbol{w}(N_t)]^T$.

To solve the parameter vector $\boldsymbol{q}$ in Eq. (7), we should ensure that the matrix $\boldsymbol{W}$ is invertible but not usually a square matrix. We can easily solve the parameter vector $\boldsymbol{q}$ in Eq. (32) by using the pseudo-inverse of the $\boldsymbol{W}$ matrix as follows:

$$\boldsymbol{q} = (\boldsymbol{W}^T \boldsymbol{W})^{-1} \boldsymbol{W}^T \boldsymbol{y}. \tag{8}$$

The parameter vector $\boldsymbol{q}$ can be calculated with a series of N_t input/output data pairs prepared for the training data [6].

B. GMDH (Group Method of Data Handling) Method

In order to solve the system problem such as control, monitoring, prediction, diagnosis and so on, a lot of mathematical methods have been studied.

The GMDH method is one of them. A GMDH model was used to predict the major transient time points accurately when LOCAs occurred. Generally, the GMDH algorithm can automatically find interrelations in the data and select the optimal structure of the model. The GMDH method which is one of the data-driven models such as ANN (Artificial Neural Network) can be used for LOCA break size prediction in this paper. Data-driven models have many advantages of easy implementation and accuracy, and famous for superior capability in modelling complex systems [7].

1. Basic GMDH algorithm

The GMDH algorithm uses a data structure similar to that of multiple regression models. The data set can be divided into the training data and test data. The reason of dividing the data set is to prevent overfitting and maintain model parsimony. Fig. 2 shows the data structure used in the GMDH method with N being the number of observations and m the number of prediction model inputs [7].

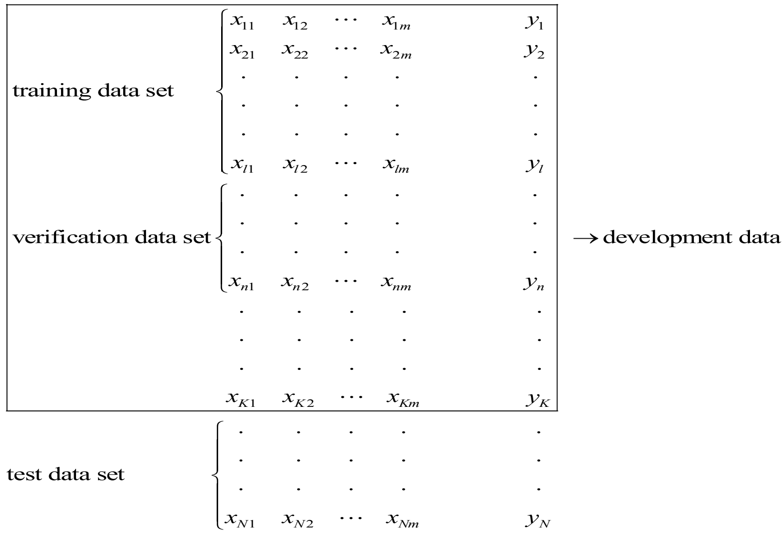

Fig. 2. GMDH data structure

Data sets from 1 to t are used for model fitting, and sets from t + 1 to n are used for overfitting check. Another approach is to use the entire data set as the checking data. The GMDH uses a self-organizing modeling algorithm with the flexibility of choosing nonlinear forms of the basic inputs $\{x_1, x_2, \cdots, x_m\}$. Figure 3 shows the branch architectures of the GMDH module, which begins with the basic inputs at the first level, and become more complicated as the number of layers increases [7].

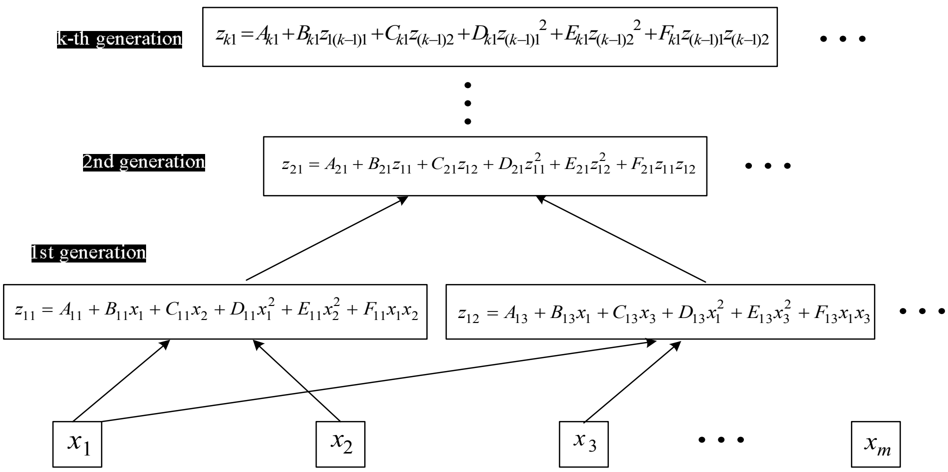

Fig. 3. Branch structure of the GMDH Model

The original GMDH method adopted the following general form at each level of the successive approximation [8]:

$$y = f(x_i, x_j) = A + Bx_i + Cx_j + Dx_i^2 + Ex_j^2 + Fx_i x_j \qquad (9)$$

Although only quadratic terms are shown in Equation (9), more complex functional forms such as ratio terms, trigonometric, logic and exponential terms, could also be incorporated as input terms according to the complexity of system.

The GMDH algorithm constructs a high-order polynomial of Kolmogorov-Gabor form. The Kolmogorov-Gabor form that is called as Ivakhnenko polynomial can be expressed as follows [8]:

$$y = a_0 + \sum_{i=1}^{m} a_i x_i + \sum_{i=1}^{m}\sum_{j=1}^{m} a_{ij} x_i x_j + \sum_{i=1}^{m}\sum_{j=1}^{m}\sum_{k=1}^{m} a_{ijk} x_i x_j x_k \cdots \qquad (10)$$

where is an input vector and is a coefficient vector that is a weight vector of Kolmogorov-Gabor polynomial. The GMDH algorithm can determine the structure of the model and also calculate the system output of the most important input simultaneously. This uses the composition of lower order polynomials mentioned above. That means the GMDH algorithm combines lower order regression type polynomials at each generation to arrive at the next generation. This process continues until the GMDH model starts to simulate the noise in training or it exceeds maximum calculation time. If an evaluation value (R) is greater than a reference value, the regression equation is fallen behind. Otherwise, the regression equation is survived. The survived regression equation value is used as a training data of the new generation. This process is conducted about all possible pairs of independent variables. The descendant with the smallest evaluation value in the evaluation of this generation is selected as the optimum fit. If the smallest evaluation value of the current generation is smaller than that of the previous generation, the above process is performed repeatedly. When overfitting of the evaluation $(R_{\min}^{G})$ value is found through alternation of generation, the process is stopped. That is, if the smallest evaluation value of the current generation is larger than that of the previous generation, the process is stopped [9].

As shown in Fig. 4, if overfitting is found, the process of the algorithm is stopped and the optimum fit of the previous generation is selected as the optimized model that predicts the LOCA size [9].

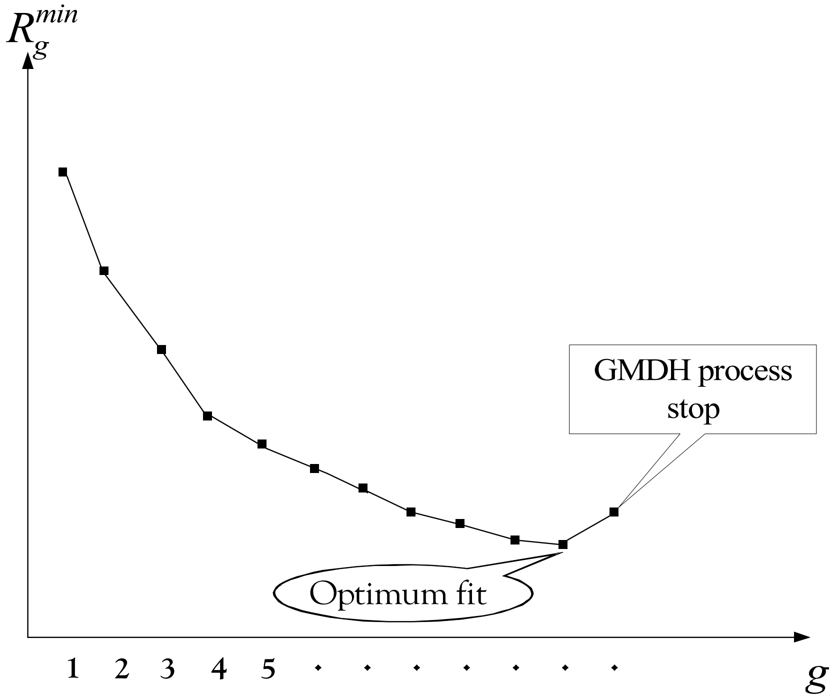

Fig. 4. Evaluation value of each generation

2. Main Implementation Steps

The GMDH algorithm has been developed and improved in many applications. The main steps in its implementation are given below.

Step 1:

Constructing the input and corresponding output data for GMDH model and dividing them into training and testing sets. Preprocessing the data in order to normalize the data set.

Step 2:

Choosing the external inputs to the GMDH network. Calculating regression polynomial parameters for each pair of input variables x and associated output y in the training sets. Least-squares error (LSE) linear regression parameters are calculated. $m(m-1)/2$ linear-regression parameters are involved in this step. Ridge regression is adopted in order to avoid the collinear problem.

Step 3:

Recalculating present layer's output using all data sets with the parameters generated in step 2. Store these outputs in a new matrix as the new input terms for the next layer of the GMDH architecture.

Step 4:

Sorting of Variables. At the completion of step 3, the algorithm designs a group of new variables $(m_g = m_{g-1}(m_{g-1}-1)/2)$ in the previous step. Here, m_g is the number of input variables for generation. A criterion is used to evaluate the new variables in the generation g and is related with the error for the checking data, which is defined as follows:

$$r_j^2 = \frac{\sum_{i=l+1}^{n} (y_i - z_{ij})^2}{\sum_{i=l+1}^{n} y_i^2} \quad \text{for } j = 1, 2, \ldots, m_g \tag{18}$$

Where j is the number of layer. Arranging the columns of Z by increasing order of r_j. An arbitrary cut-off value 'R' needs to be selected by the analyst. All the columns of Z satisfying r_j<R are picked to replace the input terms in the previous layer, and all the variables with r_j>R are screened out and are not passed on to the next generation of the algorithm.

Step 5:

Optimality test:

The process above is performed recursively until overfitting is found through cross checking; that is, when the RMSE of current layer is larger than the last layer. In detail the procedure is: the minimum value of those r_j's for generation k is denoted as $R_{\min k}$, if $R_{\min k} > R_{\min}$, then the algorithm training and testing processes stop and the polynomial with the minimum value of the error criterion in layer k-1 is selected to be the final approximate model. Otherwise, the algorithm moves to the next layer and repeats the above steps.

It has been shown that $R_{\min}$ curve has the quadratic shape, thus showing that the GMDH does converge to a global minimum value [10].

At the end of the GMDH algorithm, regression parameters are stored. The estimated coefficient for the high-order polynomial is determined by tracing back the GMDH structure until it reaches the original variables $x_1, x_2, \cdots, x_m$. As shown in Fig. 5, the tree structure with the optimum fit at the top is called an Ivakhnenko Tree [11].

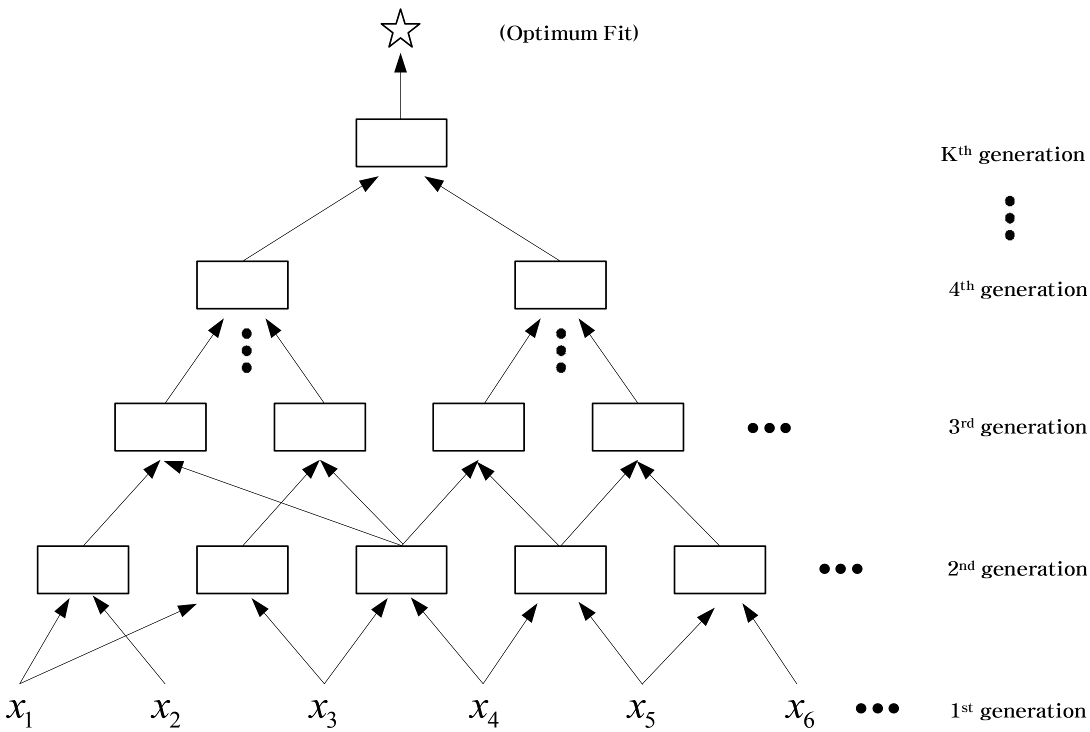

Fig. 5. Ivakhnenko tree

C. Performance Comparison of FNN and GMDH Method

A fuzzy neural network (FNN) and group method of data handling (GMDH) models were applied to predict the important timings of the LOCA (time approaching the core exit temperature exceeding 1200°F, core uncovery time, reactor vessel failure time, etc.). The input data for GMDH and FNN model is used what the integral value of the measured signal within 90 seconds after the reactor shutdown. Table 1 shows selected inputs and integrating time for the severe accident scenario of hot-leg, cold-leg, SGTR that were applied GMDH Model. And table 2 shows selected inputs and integrating time for the severe accident scenario of hot-leg, cold-leg, SGTR that were applied FNN Model.

TABLE 1. The selected inputs and integrating time of the GMDH Model

(a) Hot-leg LOCA

Scenario type	Selected inputs	Integrating time span (sec)
Core exposure time	Pressurizer water level	90
	Collapsed sump water level	30
	Collapsed water level	40
	Unbroken side S/G water temperature	60
Time that CET exceeds 1200°F	Containment pressure	30
	Containment gas temperature	90
	Pressurizer water level	50
	Collapsed water level	90
Reactor vessel failure time	Pressurizer pressure	30
	Pressurizer water level	30
	Broken side S/G water level	90

(b) Cold-leg LOCA

Scenario type	Selected inputs	Integrating time span (sec)
Core exposure time	Collapsed sump water level	30
	Collapsed water level	60
	Broken side S/G water level	30
	Broken side S/G pressure	60
	Unbroken side S/G water level	30
	Unbroken side S/G pressure	70
Time that CET exceeds 1200°F	Containment gas temperature	40
	Pressurizer pressure	90
	Unbroken side S/G water level	90
	Broken side S/G water temperature	30
Reactor vessel failure time	Containment pressure	90
	Pressurizer pressure	30
	Broken side S/G water level	90

(c) SGTR

Scenario type	Selected inputs	Integrating time span (sec)
Core exposure time	Collapsed water level	90
	Broken side S/G water level	30
	Unbroken side S/G water level	90
Time that CET exceeds 1200°F	Core exit temperature	30
	Pressurizer pressure	30
	Broken side S/G water level	30
Reactor vessel failure time	Core exit temperature	30
	Pressurizer water level	30
	Broken side S/G water temperature	30

TABLE 2. The selected inputs and integrating time of the FNN Model

(a) Hot-leg LOCA

Scenario type	Selected inputs	Integrating time span (sec)
Core exposure time	Core exit temperature	30
	Containment pressure	70
	Pressurizer water level	70
	Collapsed water level	30
	Broken side S/G pressure	30
Time that CET exceeds 1200°F	Unbroken side S/G water level	60
	Core exit temperature	30
	Containment pressure	90
	Pressurizer water level	90
	Collapsed sump water level	50
	Broken side S/G water temperature	30
Reactor vessel failure time	Core exit temperature	30
	Containment pressure	30
	Pressurizer water level	30

(b) Cold-leg LOCA

Scenario type	Selected inputs	Integrating time span (sec)
Core exposure time	Core exit temperature	30
	Containment pressure	30
	Pressurizer water level	90
	Collapsed sump water level	90
	Collapsed water level	30
	Broken side S/G pressure	30
Time that CET exceeds 1200°F	Containment gas temperature	50
	Pressurizer pressure	40
	Unbroken side S/G water temperature	90
	Broken side S/G water temperature	30
Reactor vessel failure time	Core exit temperature	30
	Containment gas temperature	90
	Pressurizer pressure	90

(c) SGTR

Scenario type	Selected inputs	Integrating time span (sec)
Core exposure time	Core exit temperature	30
	Broken side S/G pressure	30
	Unbroken side S/G water level	30
Time that CET exceeds 1200°F	Broken side S/G water level	90
	Unbroken side S/G pressure	90
	Broken side S/G water temperature	30
Reactor vessel failure time	Collapsed water level	30
	Broken side S/G water level	90
	Broken side S/G water temperature	30

Figs. 6-8 show the important timings for the severe accident scenario of hot-leg, cold-leg, SGTR that were applied GMDH Model.

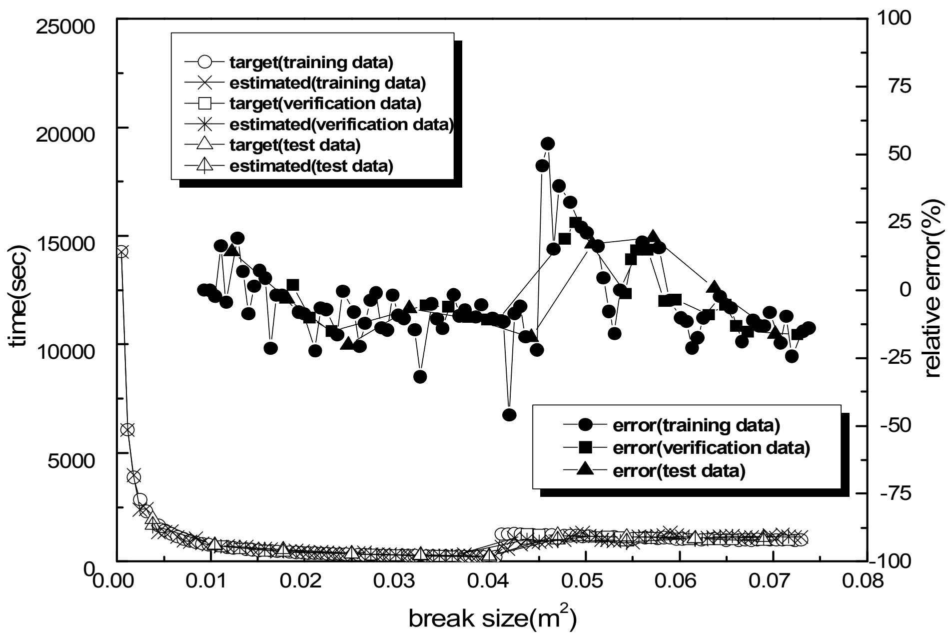

(a) Core uncovery time

Fig. 6. Prediction of the severe accident scenario in Hot-leg LOCA

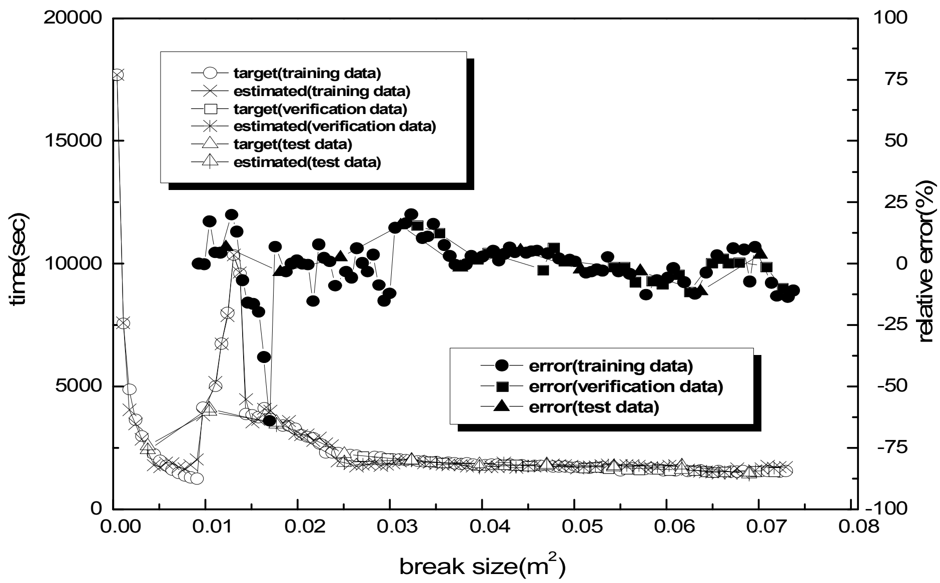

(b) Time that CET exceeds 1200°F

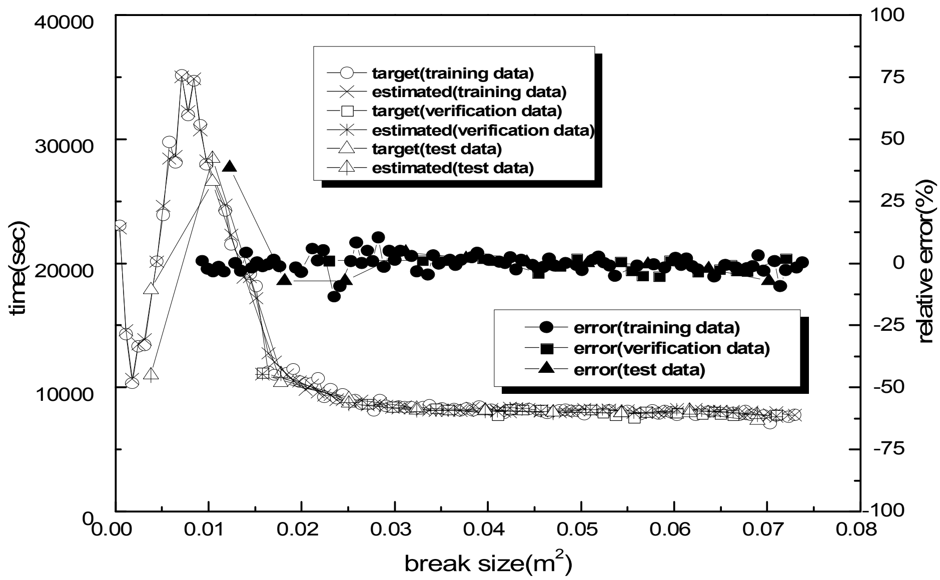

(c) RV failure time

Fig. 6. Prediction of the severe accident scenario in Hot-leg LOCA (continued)

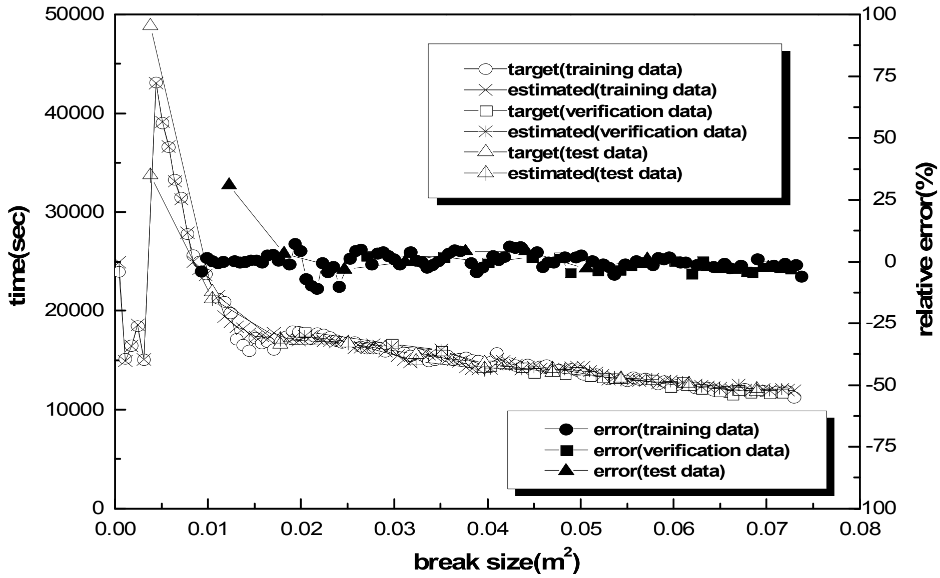

(a) Core uncovery time

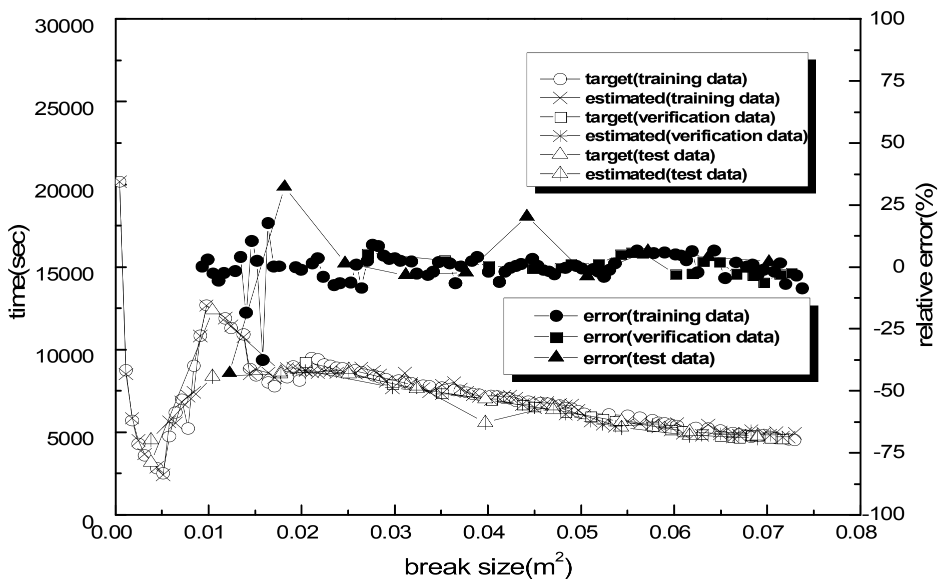

(b) Time that CET exceeds 1200°F

Fig. 7. Prediction of the severe accident scenario in Cold-leg LOCA

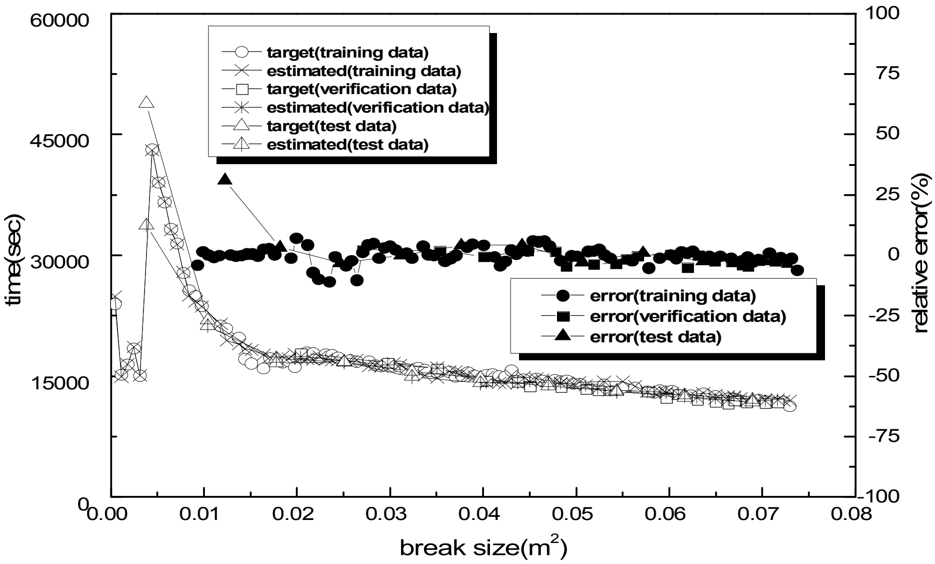

(c) RV failure time

Fig. 7. Prediction of the severe accident scenario in Cold-leg LOCA (continued)

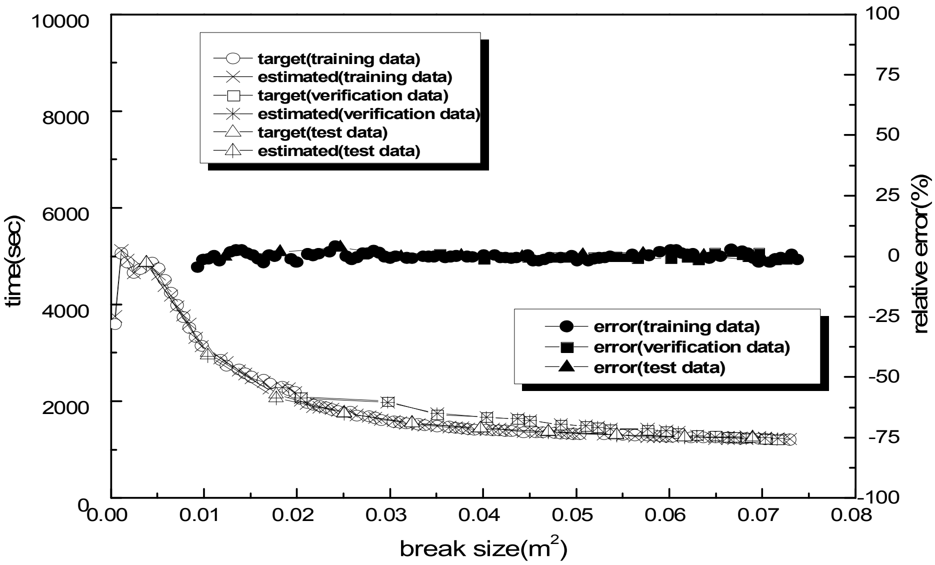

(a) Core uncovery time

Fig. 8. Prediction of the severe accident scenario in SGTR

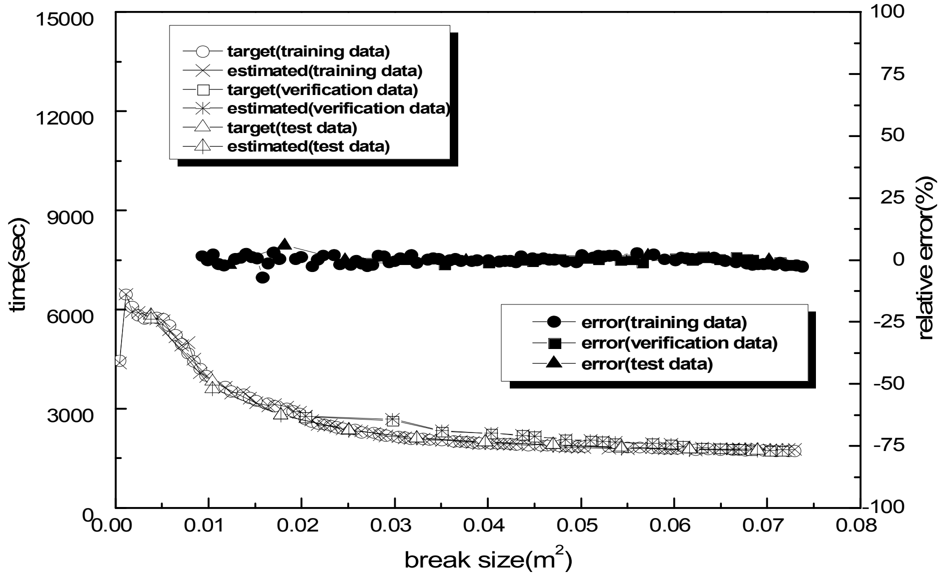

(b) Time that CET exceeds 1200°F

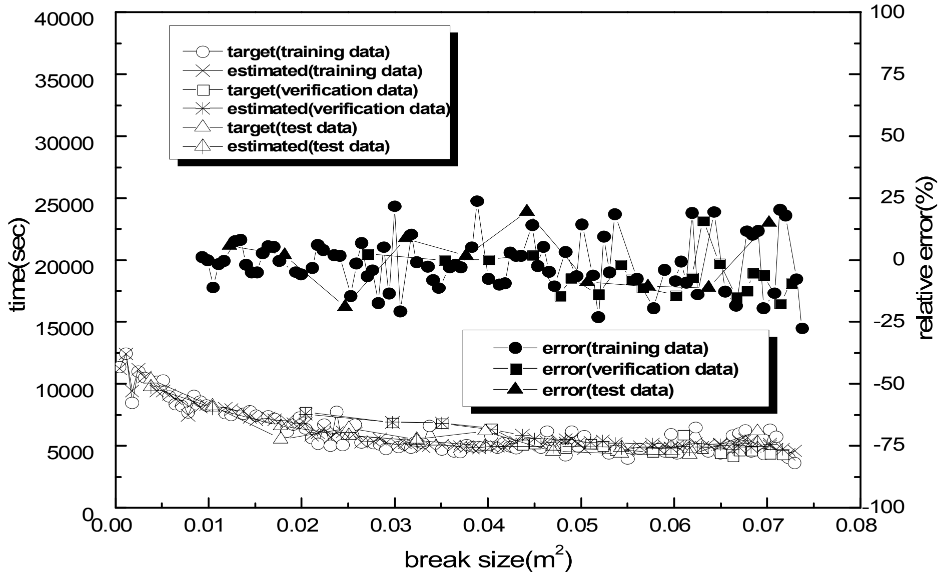

(c) RV failure time

Fig. 8. Prediction of the severe accident scenario in SGTR (continued)

Figs. 9-11 show the important timings for the severe accident scenario of hot-leg, cold-leg, SGTR that were applied FNN Model.

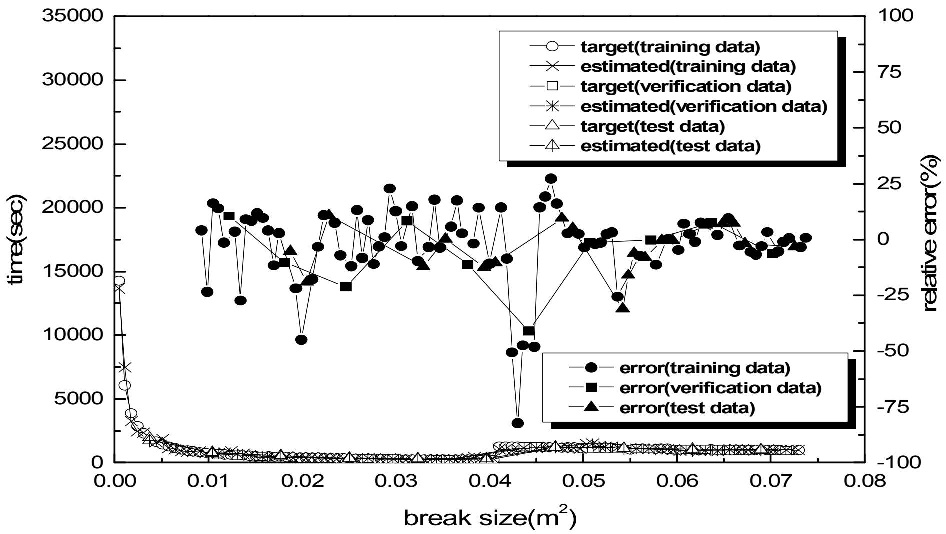

(a) Core uncovery time

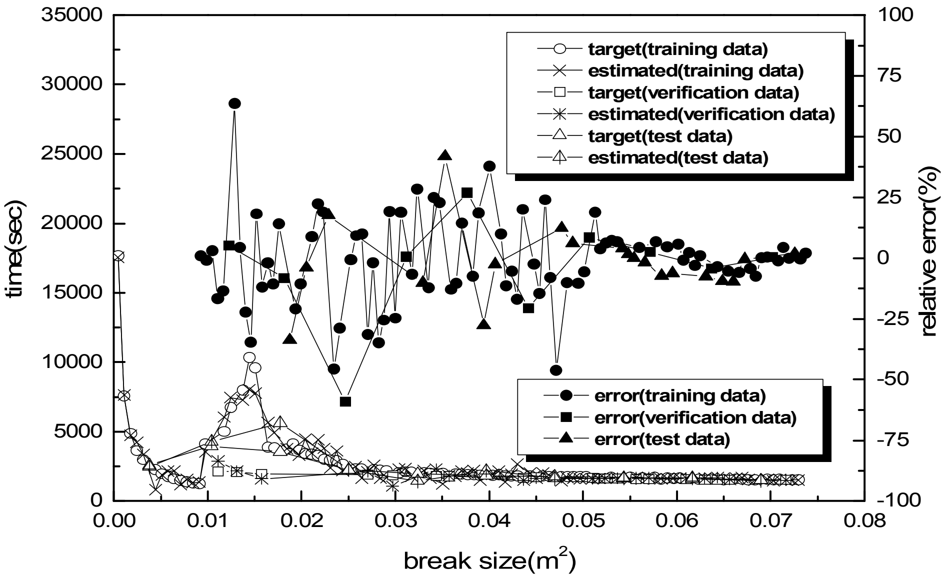

(b) Time that CET exceeds 1200°F

Fig. 9. Prediction of the severe accident scenario in Hot-leg LOCA

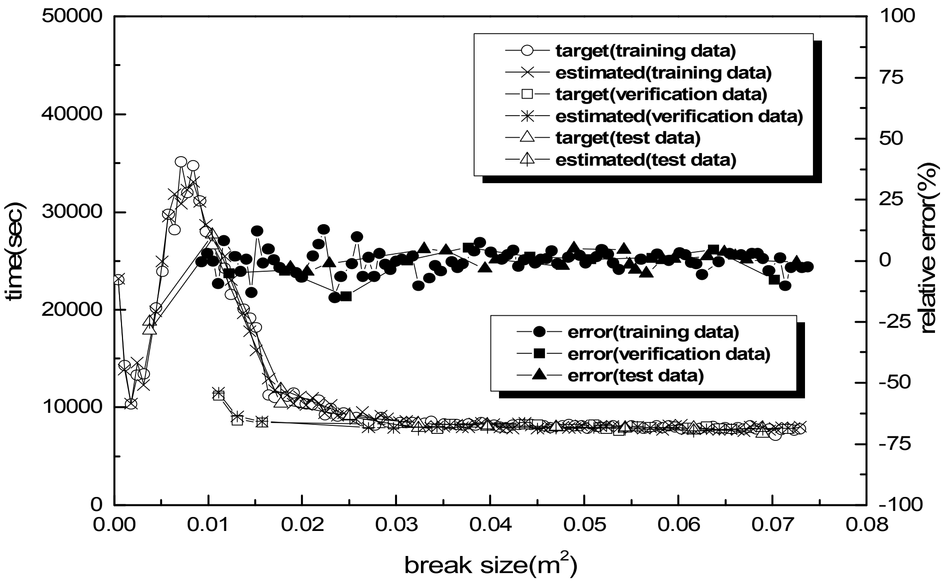

(c) RV failure time

Fig. 9. Prediction of the severe accident scenario in Hot-leg LOCA (continued)

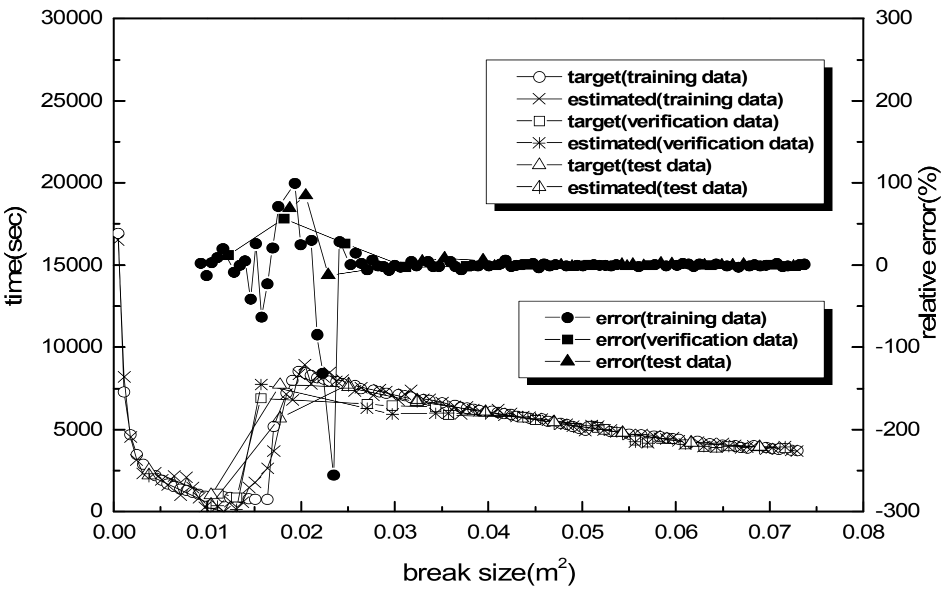

(a) Core uncovery time

Fig. 10. Prediction of the severe accident scenario in Cold-leg LOCA

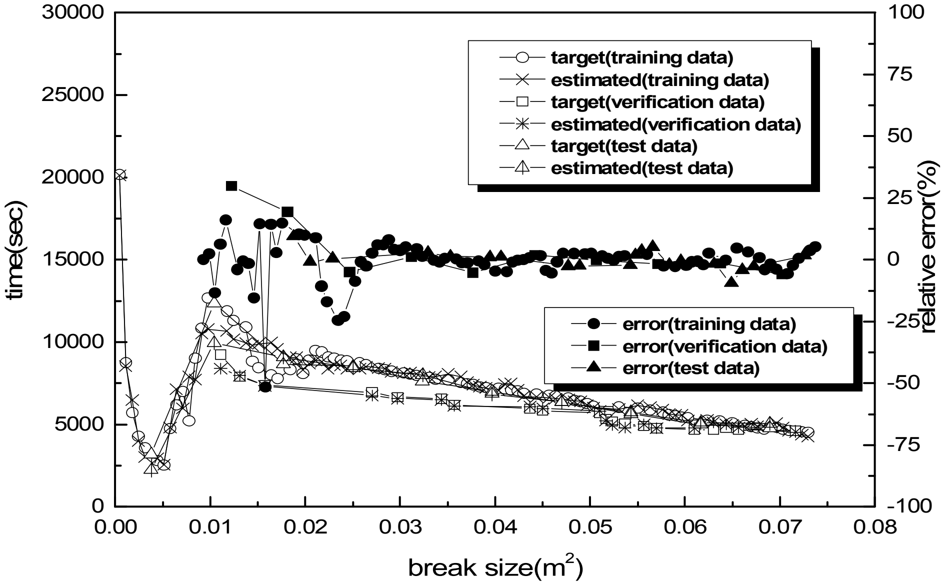

(b) Time that CET exceeds 1200°F

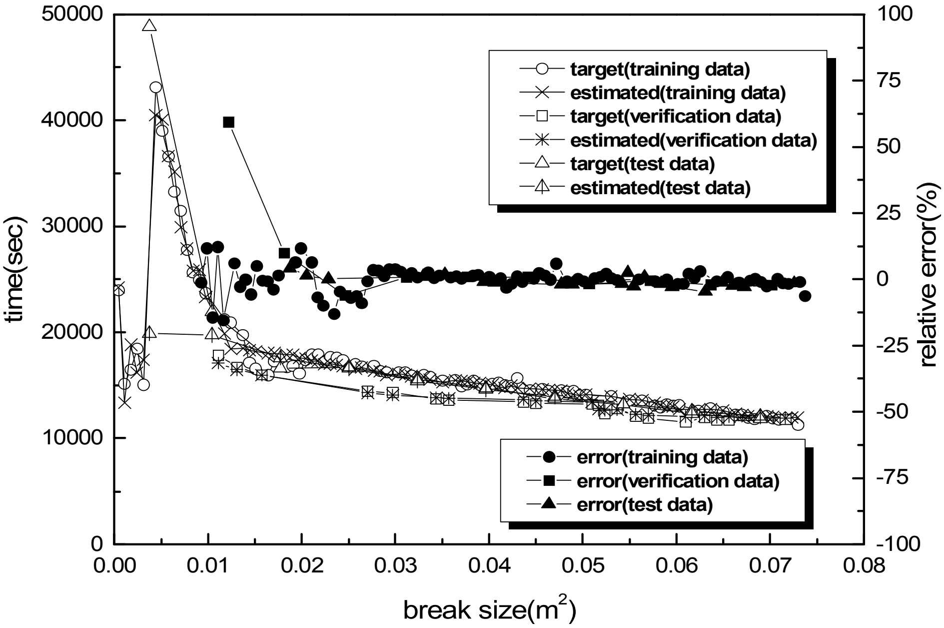

(c) RV failure time

Fig. 10. Prediction of the severe accident scenario in Cold-leg LOCA (continued)

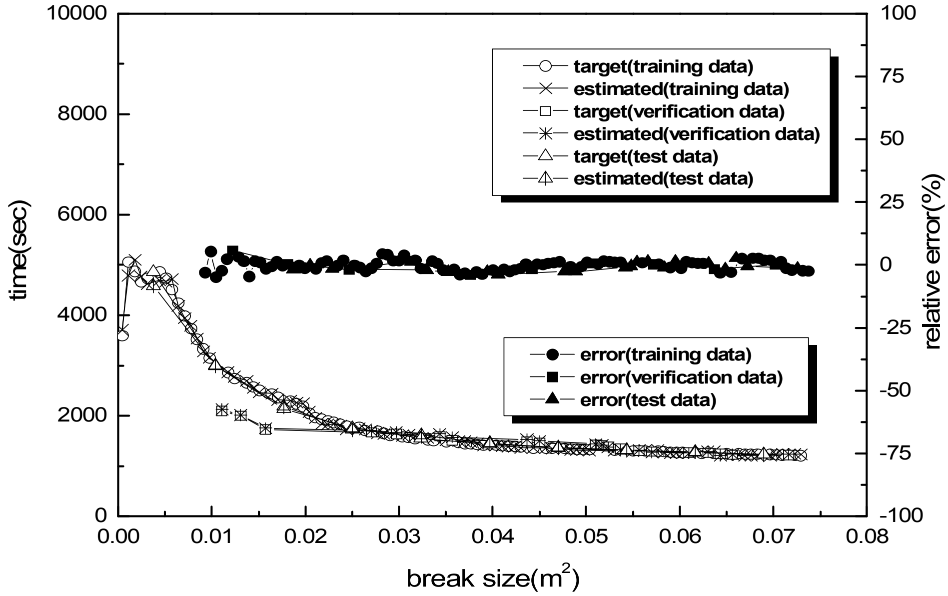

(a) Core uncovery time

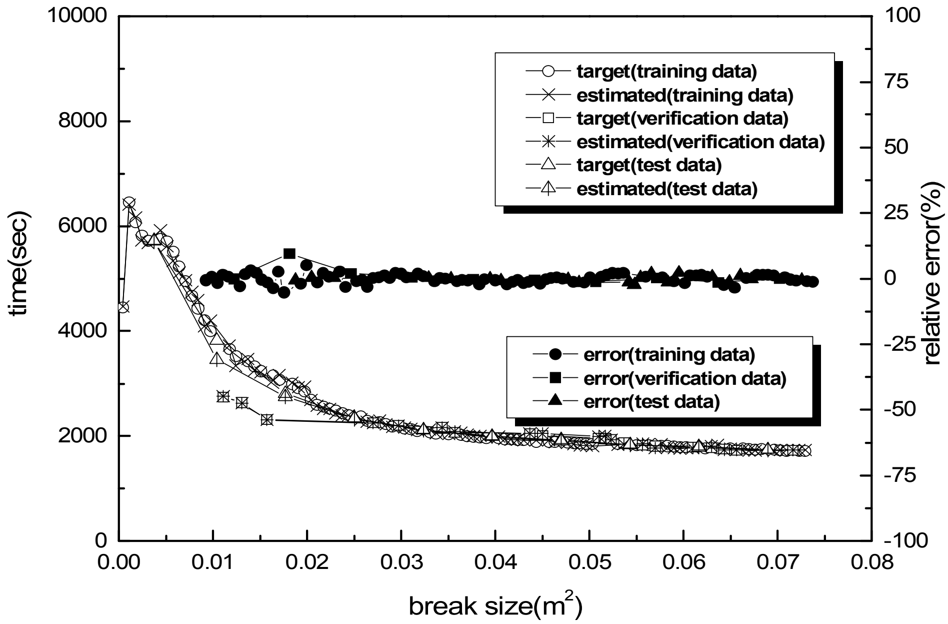

(b) Time that CET exceeds 1200°F

Fig. 11. Prediction of the severe accident scenario in SGTR

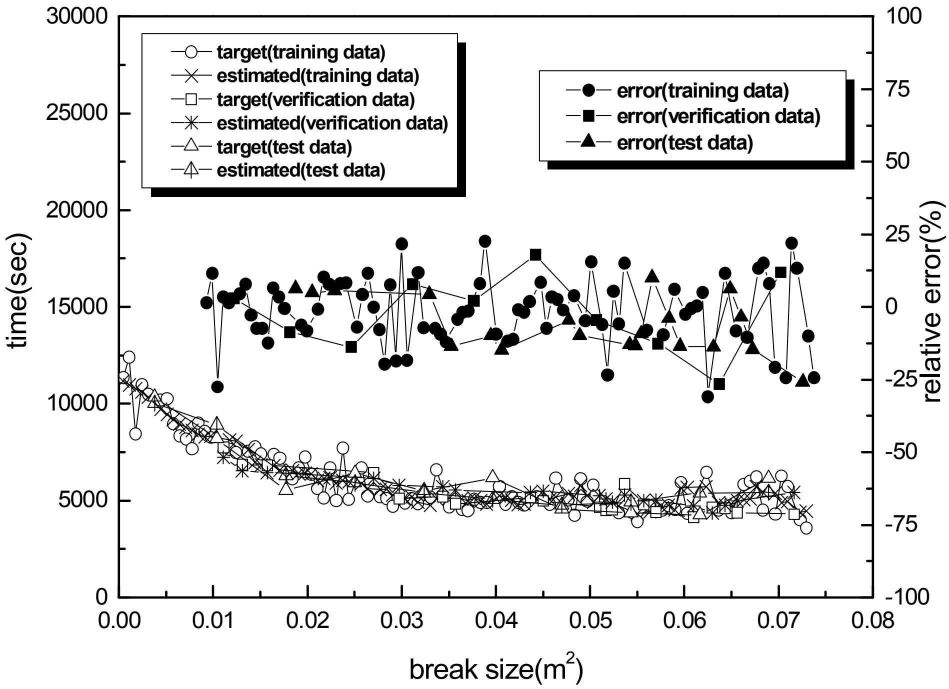

(c) RV failure time

Fig. 11. Prediction of the severe accident scenario in SGTR (continued)

Table 3 is the result of a prediction performance comparison for the GMDH and FNN model.

That shows the RMS error about the important timing of severe accidents. It is confirmed that the performance of the GMDH model is superior than the FNN model. If the GMDH model has the capability to accurately predict the core uncovery and RV failure time, it is possible to determine the recovery time of the SISs for preventing the core uncovery and RV failure.

TABLE 3. Prediction performance of the GMDH and FNN model

Initiating Event	Scenario type	GMDH model	FNN model
		RMS error(%)	RMS error(%)
Hot-leg LOCA	Core exposure time	15.7101	16.5496
	Time that CET exceeds 1200°F	10.7640	17.7667
	RV failure time	5.0384	4.7468
Cold-leg LOCA	Core exposure time	13.8685	34.6682
	Time that CET exceeds 1200°F	7.9373	8.6023
	RV failure time	4.3734	7.0943
SGTR	Core exposure time	1.3699	2.1122
	Time that CET exceeds 1200°F	1.5448	1.8323
	RV failure time	10.8637	11.6426

Ⅲ. Accident Simulation Data

The proposed model was applied to predict the LOCA break size and LOCA scenarios. To train and independently test a proposed model, it is essential to obtain the data using numerical simulations because there is little real accident data. Therefore, the training and test data of the proposed model was acquired by simulating the severe accident scenarios using the MAAP4 code regarding the OPR1000 nuclear power plant.

The simulation data was divided into the break position and break size of the loss of coolant accident (LOCA). The break position was divided into hot-leg LOCA, cold-leg LOCA and SGTR, and the break size was divided into a total of 270 steps. In addition, the simulations were performed under the conditions that the Safety Injection System (SIS) does not work properly. In accidents concerned with LOCAs, because the LOCA position and size are not detected, they must be identified and predicted. The LOCA position was identified completely and the LOCA size was predicted accurately in previous studies, with an approximately 1% error level. Therefore, the LOCA size signal, which is an input signal to the GMDH model, was assumed to be predicted from the algorithms of previous studies[].

Through the simulations, a total of 810 cases of severe accident scenarios were obtained. This data was composed of 270 pieces of hot-leg LOCA.

Ⅳ. Determination of the Recovery Time

Simulations were conducted according to break size (0.1%, 1%, ⋯ , 100%), and High Pressure and Low Pressure Safety Injection system (HPSI, LPSI) actuation status in hot-leg LOCA. It was assumed that Containment Spray System (CSS) and Recirculation (REC) mode were normally actuated.

Simulations were conducted according to break size by each case (Table 4).

Table 4. Simulation case

Case	SIT Operation	HPSI Operation	LPSI Operation	CSS Operation
1	Success	N/A	N/A	Inj & Rec
2	Success	Inj & Rec	N/A	Inj & Rec
3	Success	N/A	Inj & Rec	Inj & Rec
4	Success	Delay Inj & Rec	N/A	Inj & Rec
5	Success	N/A	Delay Inj & Rec	Inj & Rec

Fig. 12 shows the core uncovery and RV failure time of the case 1 for the severe accident scenario of hot-leg LOCA.

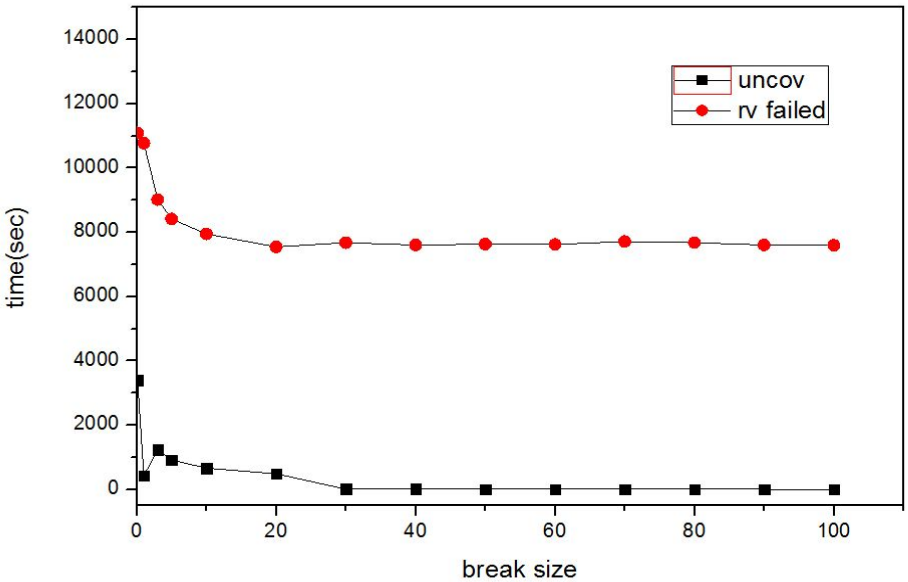

Fig. 12. Core uncovery and RV failure time of the case 1 (Hot-leg LOCA)

A. The influence of the high pressure safety injection

Fig. 13 show the core uncovery time of the case 2 for the severe accident scenario of hot-leg LOCA. In case of more than approximately 30% break area, core uncovery is occurred by the massive coolant leaks. If the HPSI is normally operated, RV failure does not occur. It is possible to prevent RV failure.

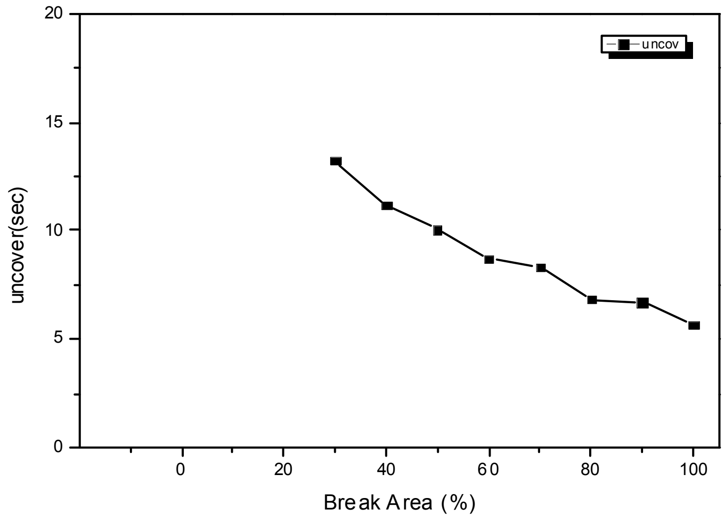

Fig. 13. Core uncovery and RV failure time of the case 2 (Hot-leg LOCA)

Table 5 shows that core uncovery does not occur in case of HPSI normal actuation in case of less than approximately 30% break area. But core uncovery is occurred by the massive coolant leaks in case of more than approximately 30% break area.

In case of less than 30% break area, it is possible to prevent core uncovery although HPSI is delayed. And we confirm recovery time for preventing core uncovery.

In case of more than 30% break area, it is possible to prevent RV failure according to the HPSI actuation time. It is recovery time for preventing RV failure.

Table 5 shows core uncovery and RV failure times according to break area and the normal actuation of HPSI and its delayed actuation in hot-leg LOCA.

TABLE 5. The influence of the high pressure safety injection in hot-leg (Case 2, 4)

Break Area Max:1.787m²	No LPSI, HPSI normal		Delay time	No LPSI, HPSI delay	
	Uncovery	RV failure		Uncovery	RV failure
0.1%	-	-	3180	3403.7	-
1%	-	-	350	435.8	-
10%	-	-	610	664.7	-
20%	-	-	440	488.1	-
30%	13.2	-	7590	13.2	7672.1
40%	11.2	-	7520	11.2	7604.5
50%	10.1	-	7550	10.1	7636
60%	8.7	-	7540	8.7	7634.1
70%	8.3	-	7620	7.7	7733.9
80%	6.9	-	7570	6.9	7762.7
90%	6.7	-	7500	6.2	7638.2
100%	6.7	-	7430	7.7	7626.5

B. The influence of the low pressure safety injection

The situation that only LPSI actuates is similar to that of HPSI, but it is different in less than 3% break area. The LPSI does not actuate normally by primary side system pressure in case of less than 3% break area.

Figs. 14 and 15 show the core uncovery and RV failure time of the case 3 for the severe accident scenario of hot-leg LOCA. In case of less than approximately 3% break area, core uncovery and RV failure are occurred. Because the LPSI does not actuate normally by primary side system pressure. If the LPSI is normally operated, RV failure does not occur in case of more than approximately 3% break area.

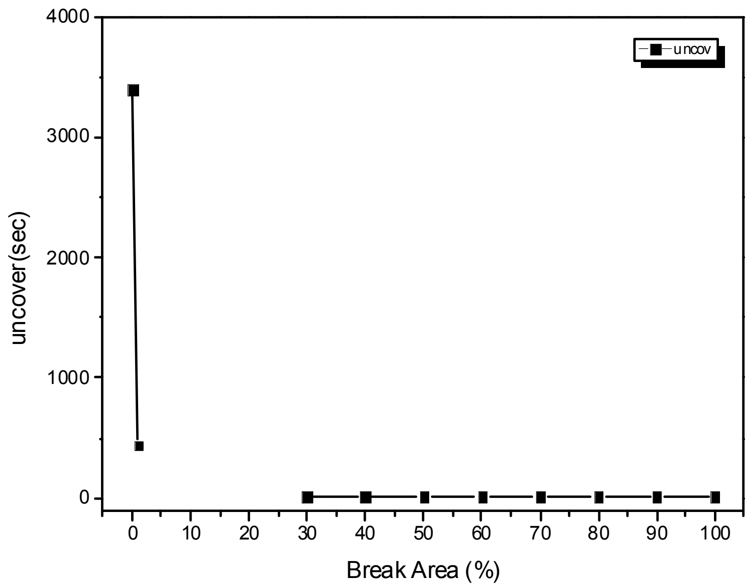

Fig. 14. Core uncovery time of the case 3 (Hot-leg LOCA)

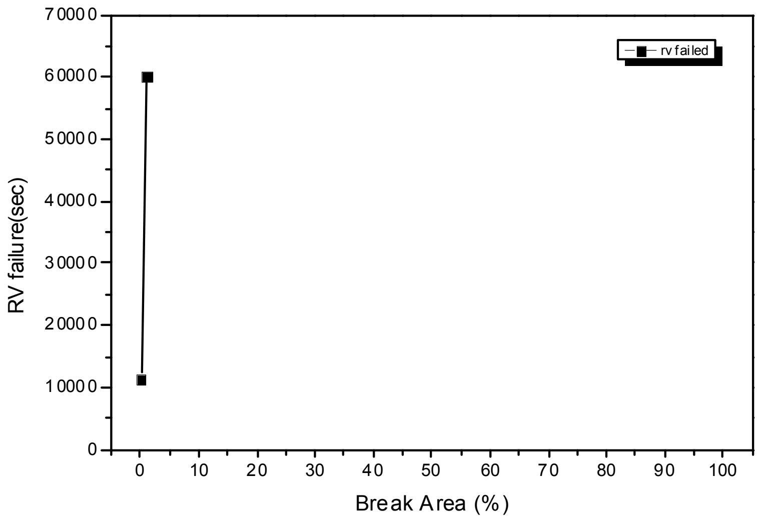

Fig. 15. RV failure time of the case 3 (Hot-leg LOCA)

Table 6 shows that core uncovery does not occur in case of LPSI normal actuation in case of less than approximately 30% break area except for less than 3% break area. But in case of more than approximately 30% break area, core uncovery is occurred by the massive coolant leaks.

In case of less than 30% break area, it is possible to prevent core uncovery although LPSI is delayed. And we confirm recovery time for preventing core uncovery.

In case of more than 30% break area, it is possible to prevent RV failure according to the LPSI actuation time. It is recovery time for preventing RV failure.

Table 6 shows core uncovery and RV failure times according to break area and the normal actuation of LPSI and its delayed actuation in hot-leg LOCA.

TABLE 6. The influence of the low pressure safety injection in hot-leg (Case 3, 5)

Break Area Max:1.787m²	No HPSI, LPSI normal		Delay time	No HPSI, LPSI delay	
	Uncovery	RV failure		Uncovery	RV failure
0.1%	3406	11320.7			
1%	435	60045			
3%	-	-	1180	1238	-
5%	-	-	860	918	-
10%	-	-	610	663.8	-
20%	-	-	440	487.2	-
30%	13.2	-	7590	13.2	7677
40%	11.2	-	7510	11.2	7607.8
50%	10.1	-	7540	10.1	7637.6
60%	8.7	-	7520	8.7	7645.3
70%	7.7	-	7600	7.7	7745.7
80%	6.9	-	7560	6.9	7706.4
90%	6.2	-	7490	6.2	7643
100%	5.7	-	7480	5.7	7611.7

Fig. 16 shows the pressure and main time points that the LPSI normally can actuate in the 1% break area. In case of less than 4,307,000 PA of primary side pressure, SIT is possible to inject after approximately 461sec. And In case of less than 1,258,000 PA of primary side pressure, the LPSI is possible to inject after approximately 802sec.

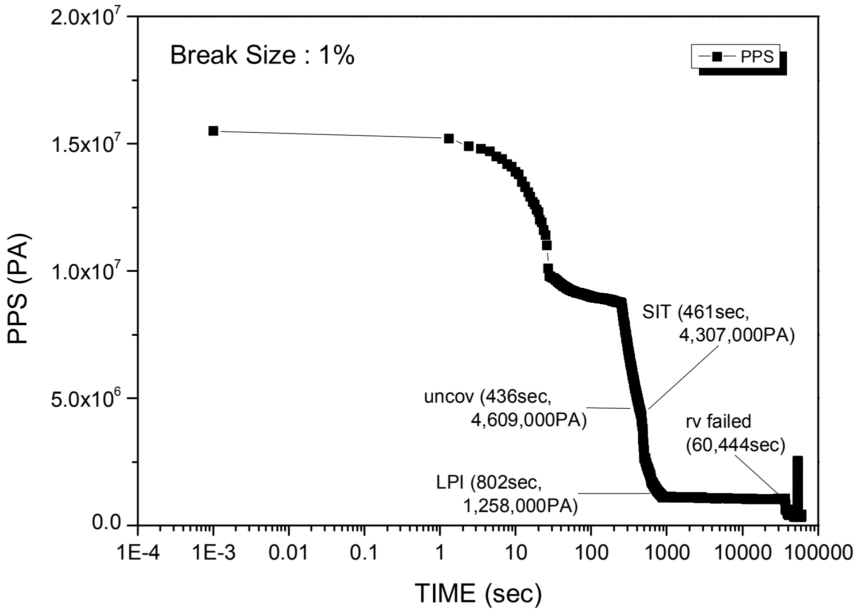

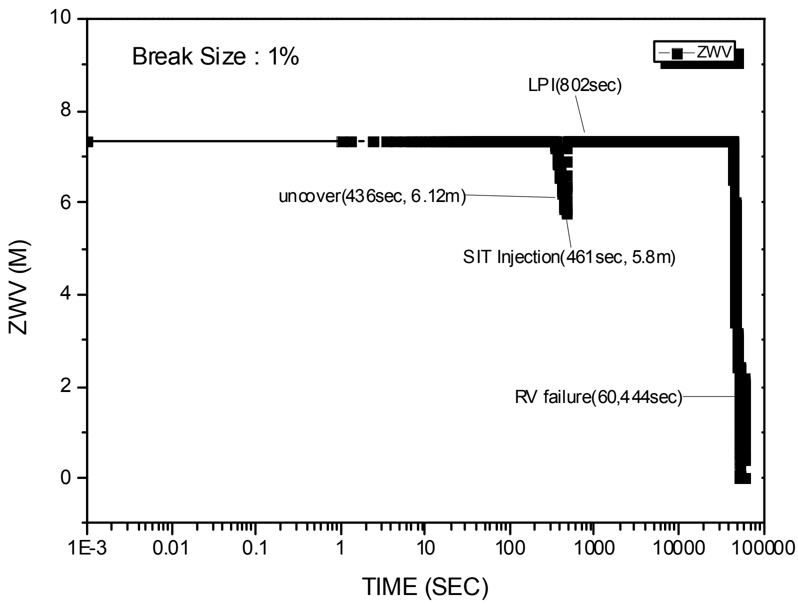

Fig. 16. Pressure and main time points

V. Conclusions

To check the status of the reactor is very important, depending on the actuation change of the safety systems. According to the previous study[4], the GMDH model has the capability to accurately predict the core uncovery time and RV failure time. The objective of this thesis is to determine the recovery time of the unhealthy safety injection systems for preventing the core uncovery and RV failure in hot-leg LOCA that may occur due to the non-actuation of SIS.

This thesis confirmed an alteration of significant timing according to the actuation status of the safety injection system through the simulations of OPR1000.

As a result of determination of the recovery time, this thesis could find the elements that interfere with the proper operation of the safety system such as pressure and time delay.

In case of less than 30% break area in hot-leg LOCA, it is possible to prevent core uncovery although the actuation of HPSI is delayed. Therefore, this thesis determined the delayed actuation time for preventing core uncovery.

In case of more than 30% break area in hot-leg LOCA, it is possible to prevent RV failure according to the HPSI actuation time although it does not prevent core uncovery. Therefore, this thesis determined the delayed actuation time for preventing RV failure.

The situation that only LPSI actuates is similar to that of HPSI, but it is different in less than 3% break area in hot-leg LOCA. Because the LPSI does not actuate normally by primary side system pressure, the core uncovery and RV failure are occurred in case of less than approximately 3% break area in hot-leg LOCA.

References

[1] Y. Bartal, J. Lin, and R. E. Uhrig, "Nuclear power plant transient diagnostics using artificial neural networks that allow "don't-know" classifications," Nucl. Technol., vol. 110, no. 3, pp. 436-449, June 1995.

[2] M. G. Na, S. M. Lee, S. H. Shin, D. W. Jung, S. P. Kim, J. H. Jeong, and B. C. Lee, "Prediction of major transient scenarios for severe accidents of nuclear power plants," IEEE Trans. Nucl. Sci., vol. 51, no. 2, pp. 313-321, April 2004.

[3] Man Gyun Na, Won Seo Park, and Dong Hyuk Lim, "Detection and Diagnostics of Loss of Coolant Accidents Using Support Vector Machines," IEEE Trans. Nucl. Sci., vol. 55, no. 1, pp. 628-636, Feb. 2008.

[4] Sung Han Lee, Young Gyu No, Man Gyun Na, Kwang-Il Ahn and Soo-Yong Park, "Diagnostics of Loss of Coolant Accidents Using SVC and GMDH Models," IEEE Trans. Nucl. Sci., vol. 58, no. 1, pp. 267-276, Feb. 2011.

[5] T. Takagi and M. Sugeno, "Fuzzy Identification of Systems and Its Applications to Modeling and Control," IEEE Trans. Systems, Man, Cybern., vol. SMC-1, no. 1, pp. 116-132, Jan./Feb. 1985.

[6] S. L. Chiu, "Fuzzy model identification based on cluster estimation," J. Intell. Fuzzy Systems, vol. 2, pp. 267-278, 1994.

[7] A. G. Ivakhnenko, "The group method of data handling; a rival of method of stochastic approximation," Soviet Automatic Control, vol. 1, no. 3, pp. 43-55, 1968.

[8] S. J. Farlow, "Self-Organizing Methods in Modeling: GMDH Type Algorithms," Marcel Dekker, New York, 1984.

[9] C. R. Hild, "Development of The Group Method of Data Handling With Information-based Model Evaluation Criteria: A New Approach to Statistical Modeling," Ph.D. Dissertation, Univ. Tennessee, Knoxville, 1998.

[10] P. B. Ferreira and B. R. Upadhyaya, Incipient Fault Detection and Isolation of Sensors and Field Devices, Nuclear Engineering Dept., Univ. Tennessee, Knoxville, UTNE/BRU/99-02, December 1999.
[11] A. G. Ivakhnenko, "Polynomial theory of complex systems", IEEE Trans. Syst. Man & Cybern, SMC-1, pp. 364-378, 1971.
[12] R. E. Henry, et al., MAAP4 - Modular Accident Analysis Program for LWR Power Plants, User's Manual, Fauske and Associates, Inc., vol. 1, 2, 3, and 4, 1990.

감사의 글

2001년도에 원자력공학과에 입학하고 2년이라는 휴학과 2년이라는 군대생활, 그리고 2009년에 늦은 학사졸업을 하게 되었습니다. 그해 8월에 지금 광주 수완지구에 위치하고 있는 열병합발전소에 취직하여 가스터빈 시운전부터 시작하여 지금 스팀터빈 운전원으로 종사하게 되었습니다.

2010년도에는 이 세상 마지막 날까지 오직 하나뿐일 사랑스런 아내와 결혼을 하게 되었고 2011년도에 원자력공학과에 다시 대학원 신입생으로 입학했습니다. 같이 신입생으로 입학한 재환이 덕분에 부담 없이 대학원생활을 잘 할 수 있을 거라고 생각했습니다. 하지만 일과 학업 그리고 가정을 함께 꾸려나가는 게 나의 마음처럼 쉽게 되지는 않고 자꾸 힘들다는 생각만 했던 게 나의 게으른 습성을 낳게 되었던 거 같습니다. 2012년에는 11월에 내 가족에 새로운 식구가 하나 늘었습니다. 나의 첫 아들!! 아빠라는 타이틀을 또 얻게 되었습니다. 나의 어깨에 책임감이 하나 더 생기고 그러고 나니 2013년에는 대리승진을 하여 조금 더 가벼워 지더니 2014년에는 둘째 아이가 생겼습니다. 계속 미뤄질 것 만 같았던 논문이 쾌한이의 도움으로 간신히 졸업논문을 완성하여 졸업을 할 수 있는 것 같습니다.

대학교 다닐 때부터 학사논문을 시작으로 대학원 입문해서 졸업때까지 못난 제자를 보듬어 주신 나만균 교수님께 머리 숙여 깊은 감사를 드립니다. 처음 대학원 입학할 때는 큰 뜻을 갖고 교수님과 상담을 했는데 졸업할 때 쯤 돼서는 교수님 앞에서 얼굴을 못들겠습니다. 바다처럼 넓은 가슴을 가지신 나만균 교수님께 다시 한번 감사를 드립니다. 그리고 조선대 원자력공학과의 스타이신 김숭평 교수님, 송종순 교수님, 정운관 교수님, 이경진 교수님, 김진원 교수님 모든 분들에게 감사를 드립니다.

그리고 나와함께 아니 거의 나를 위해 실험실을 지켜줬던 순호와 쾌한이 한테 너무 미안하고 고맙다. 각자 논문 쓰는 것도 바쁜데 내꺼 시뮬레이션 돌려주느라 고생이 많았네. 또 지금은 졸업했지만 대학원 동기 재환이도 항상 신경써줘서 고맙고 항상 잘되길 바랄게. 주현이도 이제 대전에서 일하게 돼서 축하해. 나이차가 많아서 내가 불편했었을 동영이와 주현이도 실험실 갔을 때 눈치 안줘서 고맙다.

우리 NICL 선후배님들 드디어 석사 졸업하게 되었네요. 다음 명절 모임 때는 졸업한 모습으로 보겠네요. 모일 때마다 항상 좋은 얘기해주고 서로 격려해주는 우리의 모임 아름답습니다. NICL Forever !!!!

내가 무슨 일을 하든 항상 내편이 되어주는 아은이 한테 너무 고마워요. 둘째 임신하면서 태훈이까지 키우는데 고생이 많으신 내 색시!! 앞으로 셋째까지 부탁해요.

2014년 6월 18일

김대섭